Modeling Olanzapine Solution Growth Morphologies: Supporting information

Yuanyuan Sun[1,2], Carl J. Tilbury[2], Susan M. Reutzel-Edens[3], Rajni M. Bhardwaj[3], Jinjin Li[1,], & Michael F. Doherty [2,*]*

[1]National Key Laboratory of Science and Technology on Micro/Nano Fabrication, Department of Micro/Nano Electronics, Shanghai Jiao Tong University, Shanghai 200240, China.

[2]Department of Chemical Engineering, University of California, Santa Barbara, CA 93106, United States.

[3]Eli Lilly and Company, Indianapolis, Indiana 46285, United States.

1 Mechanistic growth model

Spiral growth mechanism: The chemical potential difference between solute in solution and within the crystalline lattice is the driving force for solute crystallization out of a supersaturated solution. Crystal faces can grow via different mechanisms, but for controlled production of pharmaceuticals, layered growth mechanisms such as spiral growth and 2D nucleation are typically relevant. However, at low supersaturations, 2D nucleation events are relatively scarce and the spiral growth mechanism dominates as a self-sustaining means of growth unit incorporation. Under spiral growth, a screw dislocation provides a continuous source of step edges; growth units attach to each edge, leading to its advance across the surface. Step motion outwards from the dislocation sequentially exposes an adjacent edge, which in turn

advances after reaching a critical length l_c. This process repeats to form a spiral around the original dislocation, generating step edges that go on to complete successive crystal layers.

Periodic bond chain (PBC) theory from Hartman and Perdok[1] is used to describe the solid-state bond structure between crystal growth units. PBCs are strong, repeated interaction directions and faces of a crystal are classified as: F (flat, ≥ 2 PBCs), S (stepped, 1 PBC) or K (kinked, 0 PBCs). Generally, F faces grow via layered growth mechanisms, while S and K faces grow via rough mechanisms according to the number of favorable sites for incorporation. Growth rates for faces under rough mechanisms are 10-100 times larger than typical growth rates for faces within layered growth mechanisms,[2] leading rough faces to grow out of a crystal's shape. Thus, S and K faces can be essentially ignored when predicting the steady-state growth shape of a crystal; for F faces, each PBC is assumed to be a potential spiral side.

To calculate the spiral growth rate, the kink density along an edge must be calculated. Kink sites are the primary sites for incorporation into the crystal lattice and their distribution at thermodynamic equilibrium can be determined by Helmholtz free energy minimization[3] or Boltzmann statistics.[4] This leads to a centrosymmetric kink density of the form

$$\rho_{K,i} = \frac{2\exp\left(-\frac{\phi_i^K}{k_B T}\right)}{1 + 2\exp\left(-\frac{\phi_i^K}{k_B T}\right)} \tag{S1}$$

where ϕ_i^K is the kink energy, i.e., the energetic penalty attributed to kink formation at the step edge. The step velocity for an edge can be expressed as[5,6]

$$v_i = a_{P,i}\rho_{K,i}u_i \tag{S2}$$

where $a_{P,i}$ is the distance edge i propagates with the addition of a single row of growth units; u_i is the kink rate[6,7], which represents the net incorporation rate into a kink site. For

centrosymmetric growth units, u can be calculated from the difference between rates of attachment (j^+) and detachment (j^-) at kink sites

$$u = j^+ - j^- \tag{S3}$$

The most appropriate attachment and detachment rate expressions are[8]

$$j^+ = k^+ x = k^+ x_{sat} S \tag{S4}$$

$$j^- = k^- \tag{S5}$$

The attachment rate is first order with solute mole fraction in solution, x (which can be related to supersaturation, $S = x/x_{sat}$), while the detachment rate is zeroth order. The rate constant k^+ is normally assumed to be site-independent (i.e., depends only on solvent, but not on the specific site). The rate constant k^- depends on the bonding structure of the site (in addition to the solvent). It follows that[8]

$$k^- = k^+ \exp\left(-\frac{\Delta W}{k_B T}\right) \tag{S6}$$

where ΔW is the energy penalty for detaching a growth unit from a kink site to the solution or vapor. Thus,

$$u = k^+ \left(x_{sat} S - \exp\left(-\frac{\Delta W}{k_B T}\right)\right) \tag{S7}$$

From the equilibrium boundary condition, $u = 0$ when $S = 1$, we find

$$x_{sat} = \exp\left(-\frac{\Delta W}{k_B T}\right) \tag{S8}$$

Thus,

$$u = k^+ \exp\left(-\frac{\Delta W}{k_B T}\right)(S - 1) = k^+ x_{sat}(S - 1) \tag{S9}$$

As can be seen from Fig S1, all of the F-faces are centrosymmetric except the {1 1 0} face family. When olanzapine molecules are treated as centrosymmetric dimers, the interactions between the growth units are not completely centrosymmetric which generates the non-centrosymmetric {1 1 0} face family. For non-centrosymmetric faces, the bond structure is more complicated and the assumption of isotropic behavior on all step edges is not valid. The $[1\bar{1}1]$ and [001] edges in face {1 1 0} have two different growth units illustrated by purple and red dots in Fig. S1(d). According to the symmetry and orientation of the growth units attaching to the solid state, four different types of kink sites can exist on each edge (shown in Fig. S2), and the corresponding energetic parameters to obtain the detachment energies are reported in Table S2. From Table S2, it is seen that the kink detachment energy (ΔW^K) of growth unit B is much larger than that of growth unit A, due to larger reverse terrace energy (for more detailed information of site energy definition see ref. 7). Comparing the detachment rates j^{K-}, it can be seen that olanzapine molecules leave the crystal much faster from kink site A than kink site B, which reduces the kink rates for both $[1\bar{1}1]$ and [001] edges. The rate of olanzapine molecules leaving the crystal from terrace or edge site (j^{T-} or j^{E-}) is obtained through Eqs. S5 and S6 (since we are interested in the detachment work anisotropy, k^+ has been assigned the value of unity). The values of j^{T-} and j^{E-} at B sites are much smaller than that of j^{K-} at A sites (see highlighted values in Table S2), implying that terrace and edge attachment at B sites dominates crystal growth, and kink incorporation is not the rate-limiting step. Thus, this extreme interaction anisotropy indicates a rough growth mechanism. Given the increased density of terrace and edge sites compared to kinks, we estimate that the {1 1 0} face family has a much larger normal growth rate than the other F-faces, and is predicted to be absent from the steady-state morphology.

After obtaining the step velocity for each edge, the characteristic spiral rotation time τ_S for a convex *N*-sided polygonal spiral can be expressed as[9]

$$\tau_S = \sum_{i=1}^{N} \frac{l_{c,i+1}\sin(\alpha_{i,i+1})}{v_i} \tag{S10}$$

where $\alpha_{i,i+1}$ is the angle between edges i and $i+1$, $l_{c,i+1}$ is the critical length of edge $i+1$ and v_i is the step velocity of edge i; τ_S corresponds to the time to advance the face with a step height h in the normal direction. The critical length of edge i is given by

$$l_{c,i} = \frac{2a_{E,i}}{\ln S}\left(\frac{\phi_i^K}{k_B T}\right) \tag{S11}$$

Therefore, for the spiral mechanism, a face's growth rate can be written as

$$G = \frac{h}{\tau_S} \tag{S12}$$

Via the Frank-Chernov condition,[10,11] the steady-state crystal growth shape is given by

$$\frac{G_i}{H_i} = constant \tag{S13}$$

where H_i is the perpendicular distance of face i from the crystal center and G_i is the perpendicular growth rate of that face. Through normalizing with a reference face, the relative growth rates ($R_i = G_i/G_{ref}$) and distances ($x_i = H_i/H_{ref}$) can be related using

$$\frac{R_i}{x_i} = 1 \tag{S14}$$

Solvent effect: We studied the growth of olanzapine form I from acetone, ethyl acetate, toluene, n-butyl acetate and methyl isobutyl ketone. For crystal growth from solution, the interfacial behavior induces an energetic modification from the base solid-state interactions. Several modeling methods on the solvent-modified interactions have been systematically analyzed in our previous work.[12]

Interfacial energies on each F-face are classified into three types: terrace γ^T, edge γ^E, and kink energy γ^K (see ref. 7); the pure solute surface energies account for the solid-state

interactions that must be broken during surface formation. These interactions can be divided into dispersive and acid-base components according to the constituent force field terms. As the interfacial energy requires a per area basis, the above components are then divided by a surface area of $2a_P h$ (kink energy), $2a_E h$ (edge energy) or $2a_P a_E$ (terrace energy); note a_E is the growth unit width along the step edge.

For the solvent side, pure interfacial energies can be obtained using solubility parameters and appropriate correlations, such as[13]

$$\gamma_{solv,z} = f(V_m^{solv})^{1/3}(\delta_z)^2 \tag{S15}$$

where V_m^{solv} is the molar volume for the solvent, δ_z is the solubility parameter (e.g., dispersion, h-bonding, and polarization), and f is a scaling factor required to reproduce the experimental total solvent surface energy (these parameters are reported in Table 1).

Solvent-solute interfacial energies can then be estimated as a sum of the cohesive energy of each phase (γ_1, γ_2) minus the work of adhesion $W_{ad,12}$

$$\gamma_{12} = \gamma_1 + \gamma_2 - W_{ad,12} \tag{S16}$$

The cohesive energies include dispersive and acid-base interactions, while the work of adhesion matches interactions according to their type. In toluene, dispersive interfacial interactions dominate, so the following equation was used to obtain interfacial surface energies

$$\gamma_{solu,solv} = \gamma_{solu,dis} + \gamma_{solv,dis} + \gamma_{solu,AB} + \gamma_{solv,AB} - 2\sqrt{\gamma_{solu,dis}\gamma_{solv,dis}} \tag{S17}$$

In acetone, ethyl acetate, methyl isobutyl ketone and n-butyl acetate, the acid-base interfacial interactions between the solvent and solute molecules are considered for edges with hydrogen bonds. As the solvents selected in this work can only donate electrons, the interfacial surface energies are obtained using

$$\gamma_{solu,solv} = \gamma_{solu,dis} + \gamma_{solv,dis} + \gamma_{solu,AB} + \gamma_{solv,AB} - 2\sqrt{\gamma_{solu,dis}\gamma_{solv,dis}} - 2\sqrt{\gamma_{solu}^{+}\gamma_{solv}^{-}} \tag{S18}$$

where $\gamma_{solv}^{-} = \frac{\gamma_{solv}^{polar} + \gamma_{solv}^{H-bond}}{2}$. After obtaining the interfacial energies, ΔW is given by the specific kink/edge/terrace combination, e.g., for kink detachment,

$$\Delta W^K = 2\gamma_k^K a_P h + 2\gamma_k^E a_E h + 2\gamma_k^T a_P a_E \tag{S19}$$

Combining equations S1, S2, S9-S12, the growth rate of a F-face can be rewritten as

$$G = \left[k^+ \exp\left(-\frac{\Delta W}{k_B T}\right)\right]\left(hk_B T \sum_{i=1}^{N} \frac{a_{P,i} \exp\left(-\frac{\phi_i^K}{k_B T}\right)}{a_{E,i+1} \sin(\alpha_{i,i+1}) \phi_{i+1}^K \left(1 + \exp\left(-\frac{\phi_i^K}{k_B T}\right)\right)}\right)[\sigma \ln(1+\sigma)] \tag{S20}$$

where $\sigma = S - 1$. The face-dependent mechanistic parameters can be grouped like eq. (53) in ref 14

$$hk_B T \sum_{i=1}^{N} \frac{a_{P,i} \exp\left(-\frac{\phi_i^K}{k_B T}\right)}{a_{E,i+1} \sin(\alpha_{i,i+1}) \phi_{i+1}^K \left(1 + \exp\left(-\frac{\phi_i^K}{k_B T}\right)\right)} = \frac{h}{\tau_S^*} \tag{S21}$$

leading to

$$G = [k^+ x_{sat}]\left(\frac{h}{\tau_S^*}\right)[\sigma \ln(1+\sigma)] \tag{S22}$$

Thus, the growth rate can be grouped into three parts. The first part is solvent-dependent, the second one is face-dependent, and the third one is supersaturation-dependent.

Table S1. Force field components of the PBC bonds.

Face	Bond direction	Dispersive energy (kcal mol^{-1})	Coulombic energy (kcal mol^{-1})	Repulsive energy (kcal mol^{-1})	Total energy (kcal mol^{-1})
{1 0 0}	[001]	-8.14	0.10	2.28	-5.76
	[011]	-14.18	-5.82	5.40	-14.60
	[01 $\bar{1}$]	-14.18	-5.82	5.40	-14.60
{1 1 $\bar{1}$}	[101]	-3.88	-0.04	0.90	-3.02
	[2$\bar{1}$1]	-3.94	0.12	1.02	-2.80
	[011]	-14.18	-5.82	5.40	-14.60
{0 1 1}	[100]	-10.92	0.18	3.04	-7.70
	[2$\bar{1}$1]	-3.94	0.12	1.02	-2.80
	[01$\bar{1}$]	-14.18	-5.82	5.40	-14.60
{1 1 0}	[100]	-8.14	0.10	2.28	-5.76
	[1$\bar{1}$1]	-9.06	-2.85	3.21	-8.70
{1 2 0}	[001]	-8.14	0.10	2.28	-5.76
	[2$\bar{1}$1]	-3.94	0.12	1.02	-2.80
{0 2 0}	[100]	-10.92	0.18	3.04	-7.70
	[001]	-8.14	0.10	2.28	-5.76
	[101]	-3.88	-0.04	0.90	-3.02
{1 0 $\bar{2}$}	[211]	-3.94	0.12	1.02	-2.80
	[2$\bar{1}$1]	-3.94	0.12	1.02	-2.80

Table S2. Energetic parameters for the [001] and [1$\bar{1}$1] edges on face {1 1 0} of olanzapine form I in ethyl acetate. ϕ^K and ϕ^{RK} correspond to the kink and reverse kink energies, ϕ^E and ϕ^{RE} correspond to the edge and reverse edge energies, ϕ^T and ϕ^{RT} correspond to the terrace and reverse terrace energies; ΔW^K corresponds to the kink detachment energy ($2(\phi^{RK}+\phi^{RE}+\phi^{RT})$), ΔW^E corresponds to the edge detachment energy $2(\phi^{RE}+\phi^{RT})$, and ΔW^T corresponds to the terrace energy ($2\phi^{RT}$); j^{T-}, j^{E-}, and j^{K-} are the terrace, edge, and kink detachment rates. All energies are in kcal/mol, all rates are in s^{-1}.

Edge	Growth unit	ϕ^K	ϕ^{RK}	ϕ^E	ϕ^{RE}	ϕ^T	ϕ^{RT}	ΔW^T	ΔW^E	ΔW^K	j^{T-}	j^{E-}	j^{K-}
[001]	A	1.00	1.00	1.05	9.12	15.88	2.79	5.57	23.81	25.82	8.21×10^{-5}	3.44×10^{-18}	1.16×10^{-19}
	B	1.00	1.00	9.12	1.05	2.79	15.88	31.77	33.86	35.87	5.04×10^{-24}	1.46×10^{-25}	4.93×10^{-27}
[00$\bar{1}$]	A	1.00	1.00	9.12	1.05	15.88	2.79	5.57	7.67	9.67	8.21×10^{-5}	2.38×10^{-6}	8.05×10^{-8}
	B	1.00	1.00	1.05	9.12	2.79	15.88	31.77	50.01	52.01	5.04×10^{-24}	2.11×10^{-37}	7.12×10^{-39}
[1$\bar{1}$1] east	A	0.96	3.64	1.08	5.50	16.73	2.93	5.87	16.87	24.15	4.96×10^{-5}	4.22×10^{-13}	1.95×10^{-18}
	B	3.64	0.96	5.50	1.08	2.93	16.73	33.47	35.63	37.54	2.85×10^{-25}	7.42×10^{-27}	2.93×10^{-28}
[1$\bar{1}$1] west	A	3.64	0.96	1.08	5.50	16.73	2.93	5.87	16.87	18.79	4.96×10^{-5}	4.22×10^{-13}	1.67×10^{-14}
	B	0.96	3.64	5.50	1.08	2.93	16.73	33.47	35.63	42.90	2.85×10^{-25}	7.42×10^{-27}	3.44×10^{-32}

Table S3. Detailed results: olanzapine form I crystal grown from vapor. (For isotropic influence on centrosymmetric faces, the kink rates are all set to be 1 s^{-1} in vapor and all solvents selected)

Face	Edge	Φ (kcal/mol)	ρ	a_P (Å)	a_E (Å)	v (Å /s)	lc (Å)	α(radian)	h (Å)	R
{1 0 0}	[001]	2.88	0.015210	14.83	10.56	0.23	2619	0.95	10.21	1.00
	[011]	7.30	0.000009	8.60	9.10	0.000077	5717	0.95		
	[01 $\bar{1}$]	7.30	0.000009	8.60	9.10	0.000077	5717	1.24		
{1 1 $\bar{1}$}	[101]	1.51	0.145069	16.87	13.38	2.28	1739	0.70	7.08	4.42
	[2$\bar{1}$1]	1.40	0.158277	8.64	13.06	1.37	1573	1.25		
	[011]	7.30	0.000009	12.40	9.10	0.000111	5717	1.19		
{0 1 1}	[100]	3.85	0.002993	9.05	10.38	0.03	3442	0.77	8.50	2.08
	[2$\bar{1}$1]	1.40	0.158277	7.20	13.06	1.14	1573	0.91		
	[01$\bar{1}$]	7.30	0.000009	10.32	9.10	0.000092	5717	1.46		
{1 2 0}	[001]	2.88	0.015210	25.23	10.56	0.38	2619	1.31	6.00	≈ 10000
	[2$\bar{1}$1]	1.40	0.158277	10.20	13.06	1.61	1574	1.83		
{0 2 0}	[100]	3.85	0.002993	10.38	10.38	0.03	3442	1.39	7.41	718.82
	[001]	2.88	0.015210	10.21	10.56	0.16	2619	0.87		
	[101]	1.51	0.135069	8.06	13.38	1.09	1739	0.89		
{1 0 $\bar{2}$}	[211]	1.40	0.158277	12.20	13.06	1.93	1574	1.93	5.01	≈ 30000
	[2$\bar{1}$1]	1.40	0.158277	12.20	13.06	1.93	1574	1.21		

Table S4. Detailed results: olanzapine form I crystal grown from ethyl acetate.

Face	Edge	Φ (kcal/mol)	ρ	a_P (Å)	a_E (Å)	v(Å /s)	lc (Å)	α(radian)	h (Å)	R
{1 0 0}	[001]	1.17	0.22	14.83	10.56	3.21	1065	0.95	10.21	1.00
	[011]	2.31	0.04	8.60	9.10	0.34	1808	0.95		
	[01 $\bar{1}$]	2.31	0.04	8.60	9.10	0.34	1808	1.24		
{1 1 $\bar{1}$}	[101]	1.12	0.23	16.87	13.38	3.93	1285	0.70	7.08	1.84
	[2$\bar{1}$1]	0.46	0.48	8.64	13.06	4.14	517	1.25		
	[011]	2.31	0.04	12.40	9.10	0.48	1808	1.19		
{0 1 1}	[100]	0.96	0.28	9.05	10.38	2.56	860	0.77	8.50	2.44
	[2$\bar{1}$1]	0.46	0.48	7.20	13.06	3.45	517	0.91		
	[01$\bar{1}$]	2.31	0.04	10.32	9.10	0.40	1808	1.46		
{1 2 0}	[001]	1.17	0.22	25.23	10.56	5.47	1065	1.31	6.00	15.28
	[2$\bar{1}$1]	0.46	0.48	10.20	13.06	4.89	517	1.83		
{0 2 0}	[100]	0.96	0.28	10.38	10.38	2.93	860	1.39	7.41	11.55
	[001]	0.70	0.38	10.21	10.56	3.87	638	0.87		
	[101]	0.47	0.48	8.06	13.38	3.84	536	0.89		
{1 0 $\bar{2}$}	[211]	0.46	0.48	12.20	13.06	5.85	517	1.93	5.01	23.32

	$[2\bar{1}1]$	0.46	0.48	12.20	13.06	5.85	517	1.21		

Table S5. Detailed results: olanzapine form I crystal grown from acetone.

Face	Edge	Φ (kcal/mol)	ρ	a_P (Å)	a_E (Å)	v (Å /s)	lc (Å)	α(radian)	h (Å)	R
{1 0 0}	[001]	1.71	0.10	14.83	10.56	1.49	1553	0.95	10.21	1.00
	[011]	2.75	0.02	8.60	9.10	0.16	2156	0.95		
	$[01\bar{1}]$	2.75	0.02	8.60	9.10	0.16	2156	1.24		
$\{1\,1\,\bar{1}\}$	[101]	1.40	0.16	16.87	13.38	2.65	1618	0.70	7.08	2.02
	$[2\bar{1}1]$	0.71	0.38	8.64	13.06	3.24	801	1.25		
	[011]	2.75	0.02	12.40	9.10	0.23	2156	1.19		
{0 1 1}	[100]	1.52	0.13	9.05	10.38	1.21	1359	0.77	8.50	2.19
	$[2\bar{1}1]$	0.71	0.38	7.20	13.06	2.70	801	0.91		
	$[01\bar{1}]$	2.75	0.02	10.32	9.10	0.19	2156	1.46		
{1 2 0}	[001]	1.71	0.10	25.23	10.56	2.54	1553	1.31	6.00	17.79
	$[2\bar{1}1]$	0.71	0.38	10.20	13.06	3.83	801	1.83		
{0 2 0}	[100]	1.52	0.13	10.38	10.38	1.38	1359	1.39	7.41	11.04
	[001]	1.16	0.22	10.21	10.56	2.25	1052	0.87		
	[101]	0.73	0.37	8.06	13.38	2.97	840	0.89		
$\{1\,0\,\bar{2}\}$	[211]	0.71	0.38	12.20	13.06	4.58	801	1.93	5.01	31.71
	$[2\bar{1}1]$	0.71	0.38	12.20	13.06	4.58	801	1.21		

Table S6. Detailed results: olanzapine form I crystal grown from toluene.

Face	Edge	Φ (kcal/mol)	ρ	a_P (Å)	a_E (Å)	v (Å /s)	lc (Å)	α(radian)	h (Å)	R
{1 0 0}	[001]	0.70	0.38	14.83	10.56	5.62	639	0.95	10.21	1.00
	[011]	2.35	0.04	8.60	9.10	0.31	1843	0.95		
	$[01\bar{1}]$	2.35	0.04	8.60	9.10	0.31	1843	1.24		
$\{1\,1\,\bar{1}\}$	[101]	1.04	0.26	16.87	13.38	4.33	1198	0.70	7.08	1.71
	$[2\bar{1}1]$	0.19	0.59	8.64	13.06	5.10	218	1.25		
	[011]	2.35	0.04	12.40	9.10	0.45	1843	1.19		
{0 1 1}	[100]	0.10	0.63	9.05	10.38	5.68	91	0.77	8.50	9.55
	$[2\bar{1}1]$	0.19	0.59	7.20	13.06	4.25	218	0.91		
	$[01\bar{1}]$	2.35	0.04	10.32	9.10	0.38	1843	1.46		
{1 2 0}	[001]	0.70	0.38	25.23	10.56	9.56	639	1.31	6.00	33.06
	$[2\bar{1}1]$	0.19	0.59	10.20	13.06	6.02	218	1.83		
{0 2 0}	[100]	0.10	0.63	10.38	10.38	6.51	91	1.39	7.41	112.60
	[001]	0.06	0.64	10.21	10.56	6.57	55	0.87		

	[101]	0.17	0.60	8.06	13.38	4.85	192	0.89		
{1 0 $\bar{2}$}	[21$\bar{1}$]	0.19	0.59	12.20	13.06	7.21	218	1.93	5.01	60.88
	[2$\bar{1}$1]	0.19	0.59	12.20	13.06	7.21	218	1.21		

Table S7. Detailed results: olanzapine form I crystal grown from n-butyl acetate.

Face	Edge	Φ (kcal/mol)	ρ	a_P (Å)	a_E (Å)	v (Å /s)	lc (Å)	α(radian)	h (Å)	R
{1 0 0}	[001]	0.93	0.29	14.83	10.56	4.37	843	0.95	10.21	1.00
	[011]	2.18	0.05	8.60	9.10	0.41	1712	0.95		
	[01 $\bar{1}$]	2.18	0.05	8.60	9.10	0.41	1712	1.24		
{1 1 $\bar{1}$}	[101]	0.97	0.28	16.87	13.38	4.72	1119	0.70	7.08	1.81
	[2$\bar{1}$1]	0.35	0.53	8.64	13.06	4.55	392	1.25		
	[011]	2.18	0.05	12.40	9.10	0.59	1712	1.19		
{0 1 1}	[100]	0.74	0.37	9.05	10.38	3.31	658	0.77	8.50	2.67
	[2$\bar{1}$1]	0.35	0.53	7.20	13.06	3.79	392	0.91		
	[01$\bar{1}$]	2.18	0.05	10.32	9.10	0.49	1712	1.46		
{1 2 0}	[001]	0.93	0.29	25.23	10.56	7.44	843	1.31	6.00	16.44
	[2$\bar{1}$1]	0.35	0.53	10.20	13.06	5.37	392	1.83		
{0 2 0}	[100]	0.74	0.37	10.38	10.38	3.80	658	1.39	7.41	13.40
	[001]	0.51	0.46	10.21	10.56	4.66	467	0.87		
	[101]	0.35	0.53	8.06	13.38	4.23	404	0.89		
{1 0 $\bar{2}$}	[21$\bar{1}$]	0.35	0.53	12.20	13.06	6.42	392	1.93	5.01	24.41
	[2$\bar{1}$1]	0.35	0.53	12.20	13.06	6.42	392	1.21		

Table S8. Detailed results: olanzapine form I crystal grown from methyl isobutyl ketone.

Face	Edge	Φ (kcal/mol)	ρ	a_P (Å)	a_E (Å)	v (Å /s)	lc (Å)	α(radian)	h (Å)	R
{1 0 0}	[001]	0.70	0.38	14.83	10.56	5.61	641	0.95	10.21	1.00
	[011]	2.50	0.03	8.60	9.10	0.25	1958	0.95		
	[01 $\bar{1}$]	2.50	0.03	8.60	9.10	0.25	1958	1.24		
{1 1 $\bar{1}$}	[101]	0.68	0.39	16.87	13.38	6.57	780	0.70	7.08	2.60
	[2$\bar{1}$1]	0.29	0.55	8.64	13.06	4.76	326	1.25		
	[011]	2.50	0.03	12.40	9.10	0.35	1958	1.19		
{0 1 1}	[100]	0.87	0.31	9.05	10.38	2.84	781	0.77	8.50	2.48
	[2$\bar{1}$1]	0.29	0.55	7.20	13.06	3.96	326	0.91		
	[01$\bar{1}$]	2.50	0.03	10.32	9.10	0.30	1958	1.46		
{1 2 0}	[001]	0.70	0.38	25.23	10.56	9.54	641	1.31	6.00	37.88
	[2$\bar{1}$1]	0.29	0.55	10.20	13.06	5.62	326	1.83		
{0 2 0}	[100]	0.87	0.31	10.38	10.38	3.26	781	1.39	7.41	18.86

	[001]	0.57	0.43	10.21	10.56	4.43	515	0.87		
	[101]	0.31	0.54	8.06	13.38	4.37	356	0.89		
$\{1\ 0\ \bar{2}\}$	[211]	0.29	0.55	12.20	13.06	6.72	326	1.93	5.01	50.06
	$[2\bar{1}1]$	0.29	0.55	12.20	13.06	6.72	326	1.21		

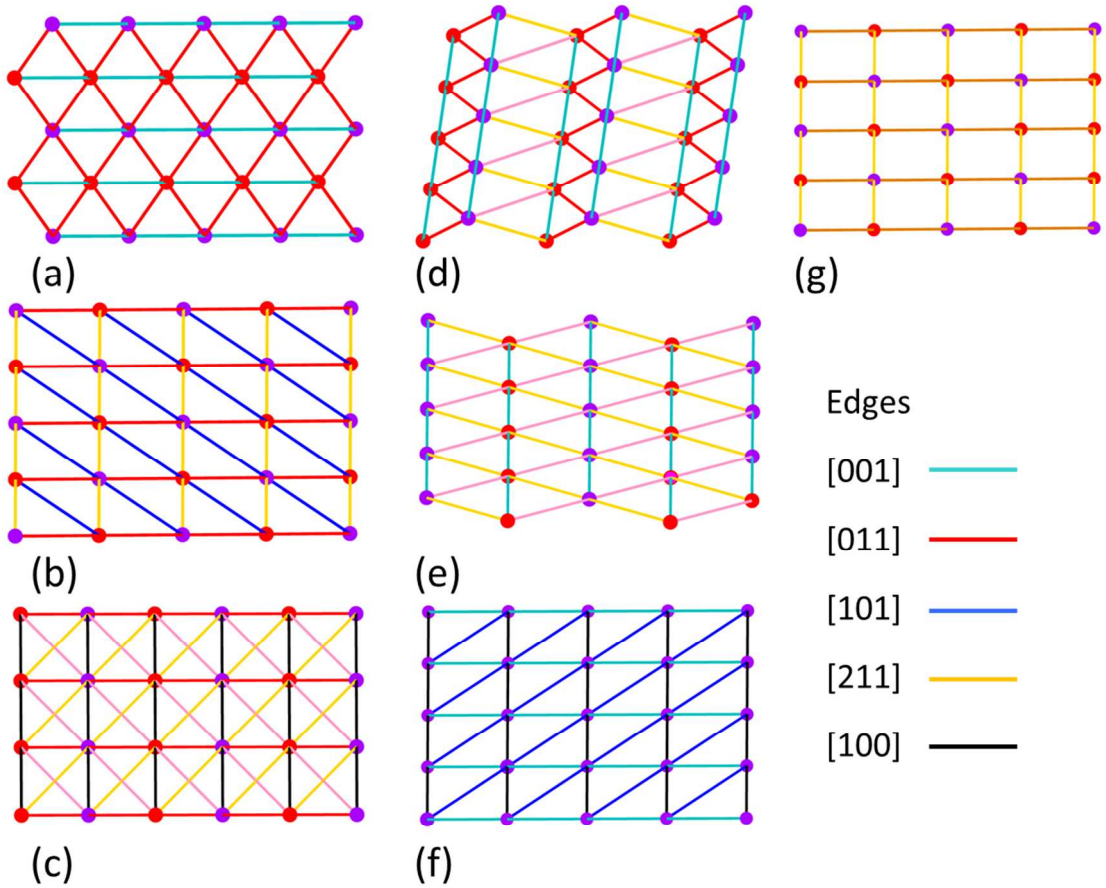

Figure S1. Bonding structures of different F-faces for olanzapine dimers (a) {1 0 0} face, (b) {1 1 $\bar{1}$} face, (c) {0 1 1} face, (d) {1 1 0} face, (e) {1 2 0} face, (f) {0 2 0} face, and (g) {1 0 $\bar{2}$} face

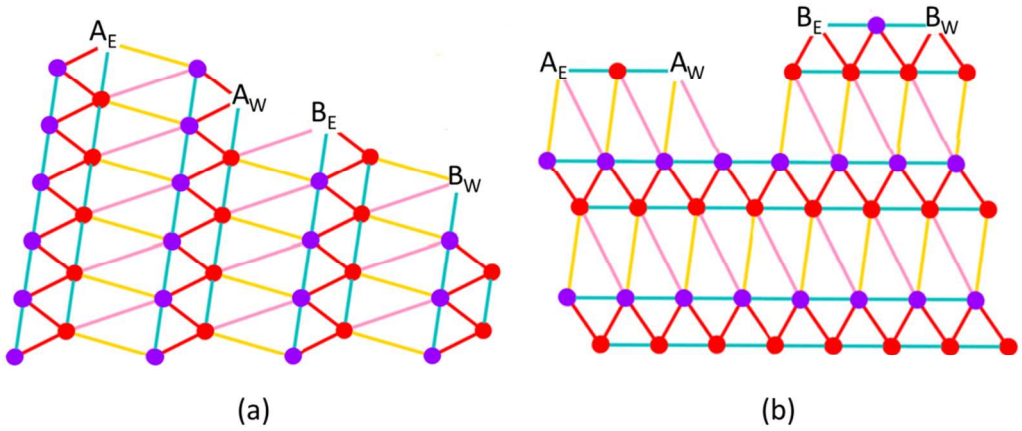

Figure S2. Four types of kink sites on [1$\bar{1}$1] edge (a) and [001] edge (b) on face {1 1 0}.

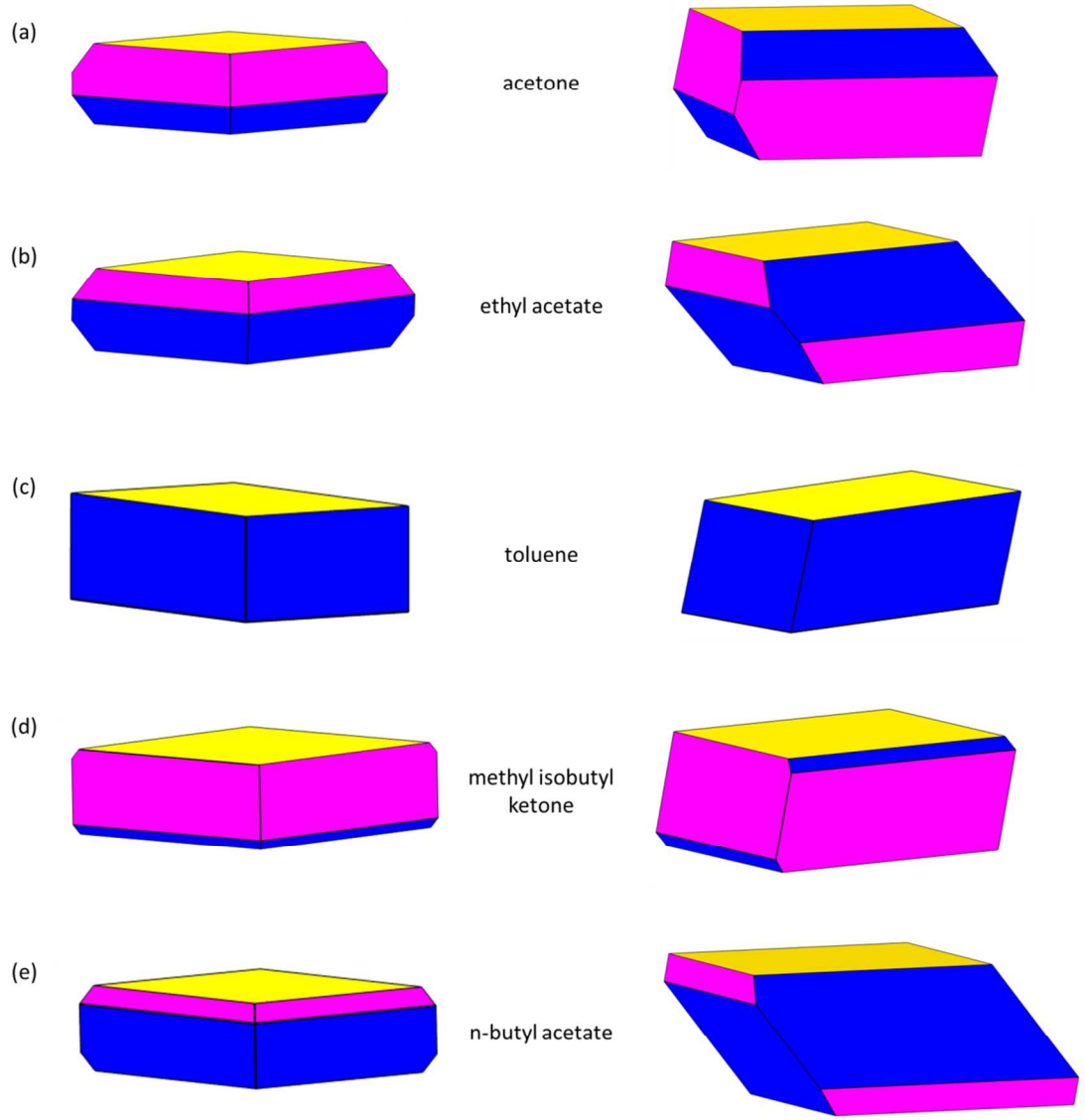

Figure S3. Two views of the predicted crystal shape grown from (a) acetone, (b) ethyl acetate, (c) toluene, (d) methyl isobutyl ketone and (e) n-butyl acetate.

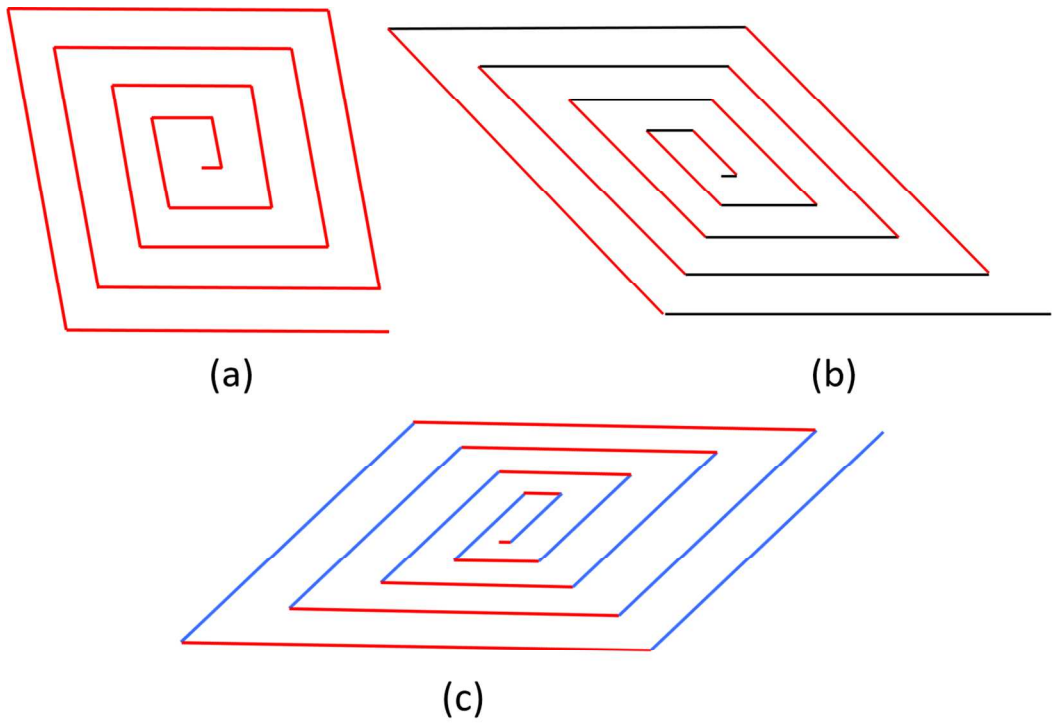

Figure S4. Predicted spirals on F-faces (a) {1 0 0}, (b) {0 1 1} and (c) {1 1 $\bar{1}$} grown from the vapor. Color coding is the same as Figure S1.

References

1. Hartman, P.; Perdok, W. G. On the Relations between Structure and Morphology of Crystals. II. *Acta Crystallogr.* **1955**, *8*, 521-524.

2. Lovette, M. A.; Browning, A. R.; Griffin, D. W.; Sizemore, J. P.; Snyder, R. C.; Doherty, M. F. Crystal Shape Engineering. *Ind. Eng. Chem. Res.* **2008**, *47*, 9812-9833.

3. Frenkel, J. On the Surface Motion of Particles in Crystals and the Natural Roughness of Crystalline Faces. *J Phys (Moscow).* **1945**, *9*, 392-398.

4. Burton, W. K.; Cabrera, N.; Frank, F. C. *Philos Trans R Soc, A.* **1951**, *243*, 299-358.

5. Kim, S. H.; Dandekar, P.; Lovette, M. A.; Doherty, M. F. Kink Rate Model for the General Case of Organic Molecular Crystals. *Cryst. Growth Des.* **2014**, *14*, 2460-2467.

6. Kuvadia, Z. B.; Doherty, M. F. Spiral Growth Model for Faceted Crystals of Non-centrosymmetric Organic Molecules Grown from Solution. *Cryst. Growth Des.* **2011**, *11*, 2780-2802.

7. Tilbury, C. J.; Joswiak, M. N.; Peters, B.; Doherty, M. F. Modeling Step Velocities and Edge Surface Structures during Growth of Non-Centrosymmetric Crystals. *Cryst. Growth Des.* **2017**, *17*, 2066-2080.

8. Li, J.; Tilbury, C. J.; Joswiak, M. N.; Peters, B.; Doherty, M. F. Rate Expressions for Kink Attachment and Detachment During Crystal Growth. *Cryst. Growth Des.* **2016**, *16*, 3313-3322.

9. Snyder, R. C.; Doherty, M. F. Predicting Crystal Growth by Spiral Motion. *Proc. R. Soc. London, Ser. A.* **2009**, *465*, 1145-1171.

10. Chernov, A. A. Crystal Growth Forms and Their Kinetic Stability. *Sov. Phys. Cryst.* **1963**, *7*, 728-730.

11. Frank, F. C. In: *Growth and Perfection of Crystals*; Doremus, R. H.; Roberts, B. W.; Turnbull, D. Eds.; Wiley: New York, 1958.

12. Tilbury, C. J.; Green, D. A.; Marshall, W. J.; Doherty, M. F. Predicting the Effect of Solvent on the Crystal Habit of Small Organic Molecules. *Cryst. Growth Des.* **2016**, *16*, 2590-2604.

13. Kaelble, D. H. *Physical Chemistry of Adhesion*; Wiley-Interscience: Hoboken, NJ, 1971.

14. Tilbury, C. J.; Doherty, M. F. Modeling Layered Crystal Growth at Increasing Supersaturation by Connecting Growth Regimes. *AIChE J.* **2017**, *63*, 1338-1352.